Convergent Synthesis and Photoinduced Processes in Multi-Chromophoric Rotaxanes

ARTICLE *in* THE JOURNAL OF PHYSICAL CHEMISTRY B · NOVEMBER 2010

Impact Factor: 3.3 · DOI: 10.1021/jp101154k · Source: PubMed

Convergent Synthesis and Photoinduced Processes in Multi-Chromophoric Rotaxanes†

Jackson D. Megiatto, Jr.,‡ Ke Li,‡,⊥ David I. Schuster,*,‡ Amit Palkar,§,# M. Ángeles Herranz,§ Luis Echegoyen,§ Silke Abwandner,|| Gustavo de Miguel,|| and Dirk M. Guldi||

Department of Chemistry, New York University, New York, New York 10003, Department of Chemistry, Clemson University, Clemson, South Carolina 29634, and Department of Chemistry and Pharmacy and Interdisciplinary Center for Molecular Materials, Friedrich-Alexander-Universität Erlangen-Nürnberg, 91058 Erlangen, Germany

Received: February 5, 2010; Revised Manuscript Received: April 20, 2010

A series of [2]rotaxane materials, in which [60]fullerene is linked to a macrocycle and ferrocene (Fc) moieties are placed at the termini of a thread, both of which possess a central Cu(I)−1,10-phenanthroline $[Cu(phen)_2]^+$ complex, were synthesized by self-assembly using Sauvage metal template methodology. Two types of threads were constructed, one with terminal ester linkages, and a second with terminal 1,2,3-triazole linkages derived from Cu(I)-catalyzed "click" 1,3-cycloaddition reactions. Model compounds lacking the fullerene moiety were prepared in an analogous manner. The ability of the interlocked $Fc-[Cu(phen)_2]^+-C_{60}$ hybrids to undergo electron transfer upon photoexcitation in benzonitrile, dichloromethane, and *ortho*-dichlorobenzene was investigated by means of time-resolved fluorescence and transient absorption spectroscopy, using excitation wavelengths directed at the fullerene and $[Cu(phen)_2]^+$ subunits. The energies of the electronic excited states and charge separated (CS) states that might be formed upon photoexcitation were determined from spectroscopic and electrochemical data. These studies showed that MLCT excited states of the copper complex in the fullerenerotaxanes were quenched by electron transfer to the fullerene in benzonitrile, resulting in charge separated states with oxidized copper and reduced fullerene moieties, $(Fc)_2-[Cu(phen)_2]^{2+}-C_{60}^{\bullet-}$. Even though electron transfer from Fc to the oxidized copper complex is predicted to be exergonic by 0.16 to 0.20 eV, no unequivocal evidence in support of such a process was obtained. The conclusion that Fc plays no role in the photoinduced processes in our systems rests on the lack of enhancement of the lifetime of the charge separated state, as measured by decay of $C_{60}^{\bullet-}$ at ∼1000 nm, since one-electron oxidized Fc is very difficult to detect spectroscopically in the 500−800 nm spectral region.

Introduction

Self-assembly has proven to be an attractive strategy for constructing fascinating and complex supramolecular systems for various purposes.[2] Diverse approaches based on hydrogen bonding, Coulombic interactions and metal complexation, have been widely utilized to assemble supramolecular architectures in which organization of the components has been achieved beyond the simple molecular level.[3]

Supramolecular systems are omnipresent in nature where they perform functions essential to life, such as photosynthesis, vision, and respiration. More specifically, light energy conversion involved in natural photosynthesis is accomplished by means of a suitably organized supramolecular system, in which the proper spatial organization of electron donor (D) and acceptor (A) moieties is achieved through noncovalent interactions. A cascade of vectorial energy and electron transfer processes generate a long-lived charge separated state $D^{\bullet+}-A^{\bullet-}$, thereby transforming the energy of the incident excitation light into redox-related chemical potential.[4]

Recent progress made in molecular recognition and self-assembly processes has allowed the preparation of complex photoactive arrays, in which the D−A moieties are noncovalently linked.[5] Among the supramolecular concepts applied in constructing artificial photosynthetic systems, metal coordination is particularly promising since in most cases transition metal complexes not only serve as building blocks to assemble the supramolecular system but also act as electronic relays, facilitating long-range electron and energy transfer processes.[6]

A number of D−A arrays have been prepared in which the active components are linked through metal coordination.[7] Among the most promising supramolecular architectures are interlocked molecules, specifically rotaxanes and catenanes.[5k,8] Rotaxanes consist of a ring threaded on a rod, in which the system is held in place by two bulky end groups, while catenanes consist of two or more interlocked rings. Their unique mechanical arrangement, in which constituent groups are located within a set distance without any direct covalent linkage, allows the components to undergo submolecular motions by application of an external stimulus.[8]

Recent developments in the synthesis of rotaxanes and catenanes at NYU have allowed the preparation of new families of organic−inorganic hybrids, where the organic subunits are zinc(II) porphyrins (ZnP) and fullerenes (C_{60}), while the inorganic component is a transition metal complex.[9] Due to the complementary photophysical properties of ZnP (electron donor) and C_{60} (electron acceptor), photoinduced energy and electron transfer processes can occur between the mechanically linked

† Part of the "Michael R. Wasielewski Festschrift".

* Corresponding author. E-mail: david.schuster@nyu.edu.
‡ New York University.
§ Clemson University.
|| University of Erlangen-Nürnberg.
⊥ Present address: DuPont Central Research & Development, Wilmington DE 19880.
Present address: ConocoPhillips, Bartlesville Research Center, Bartlesville OK 74004.

10.1021/jp101154k
Published on Web 06/02/2010

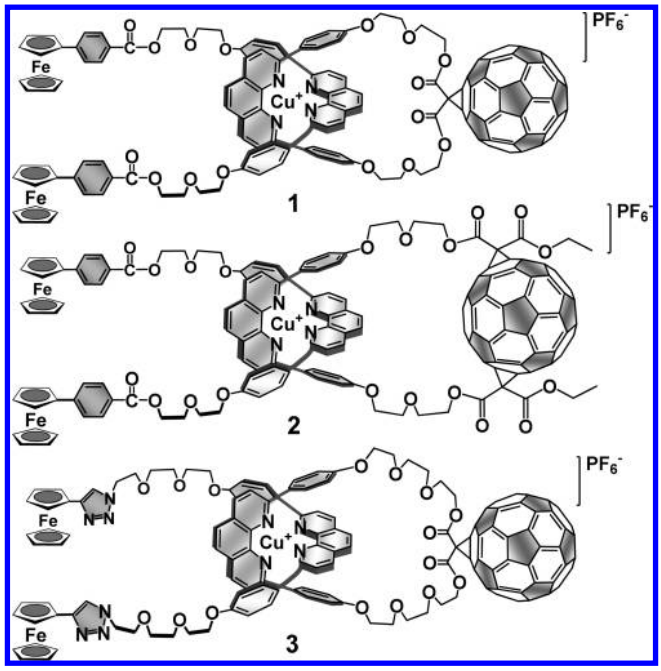

Figure 1. New family of fullerene/ferrocenyl $(Fc)_2-[Cu(phen)_2]^+-C_{60}$ rotaxanes. The size and structure of the macrocycle and the thread have been varied to study the correlation between interchromophoric distance and electron transfer dynamics.

organic and inorganic subunits.[7f,9] Addressing light excitation to a given molecular component by choice of excitation wavelength has enabled the assignment of specific roles to each entity in the hybrid structure and allowed the study of the dynamics of the light induced processes.

Our previous studies of porphyrin-fullerene based [2]rotaxanes with polyether linkages,[9] assembled by the Cu(I) template-directed method pioneered by Sauvage and co-workers,[10] have shown that upon excitation of the porphyrin subunit, a sequence of energy and electron transfer processes takes place through the (1,10-phenanthroline)$_2$−Cu(I) ($[Cu(phen)_2]^+$) complex used initially for rotaxane preparation. These photoinduced cascade events ultimately yield a long-lived charge separated (CS) state $ZnP^{\bullet+}-Cu(phen)_2]^+-C_{60}^{\bullet-}$, which is characterized by oxidized porphyrin and reduced fullerene moieties. Lifetimes of these CS states as high as 32 μs have been measured in solution at ambient temperatures.[9b]

A natural extension of this work is to introduce other electron donors into the C_{60}-based rotaxanes, with the ultimate goal of prolonging the lifetime of the charge separated states. Ferrocene (Fc) is a very good electron donor with a low oxidation potential ($E_{1/2}$ = +0.5 V vs SCE),[11] and has frequently been used in fullerene-based D−A systems as the ultimate electron donor, to generate long distance long-lived charge separated states.[12] It was therefore a logical next step in our research to incorporate Fc into rotaxanes with the expectation that multistep electron transfer reactions would take place upon electronic excitation at appropriate wavelengths, as in numerous previously studied covalent Fc−C_{60} dyads and triads,[12a−f] to generate long-distance long-lived charge separated radical pair (CSRP) states.

In the present paper, we describe two convergent synthetic strategies based on the Cu(I)-template approach for the preparation of D−A rotaxanes possessing C_{60} and Fc subunits. These target $(Fc)_2-[Cu(phen)_2]^+-C_{60}$ rotaxanes are shown in Figure 1. Both strategies have proven to be very efficient synthetic tools, affording rotaxanes in very high yields (>92% in one case). In the present work, the lengths and structure of both the axle and the ring components of the Fc−C_{60} rotaxanes were altered to achieve better understanding of the relationship between molecular topology and interchromophoric separation distance on the rates of forward and back electron transfer processes.

To better understand the photoinduced processes in this new family of rotaxanes, their photophysical properties were compared with those of analogous pseudorotaxane and rotaxane model compounds **4**−**7** shown in Figure 2, lacking the C_{60} and/or Fc moieties. These materials were synthesized using similar methodology.

Results and Discussion

1. Synthetic Design. The basic strategy we used to assembly the rotaxanes relied on three steps (see strategy A, Scheme 1). First, a phenanthroline (phen) based macrocycle was prepared, to which C_{60} was attached following classical fullerene chemistry. Second, a "threading" reaction of a phen-containing string-like fragment through the C_{60}−macrocycle, promoted by binding to the Cu(I) center,[10] generated a pseudorotaxane precursor. The pseudorotaxane was then subjected to "stoppering reactions" using ferrocene moieties, affording D−A dyads and model systems with rotaxane topologies.

To prepare the rotaxane dyads **1** and **2** shown in Figure 1, we designed an alternative approach based on the Cu(I) template methodology (see strategy B, Scheme 1). In this approach, the traditional sequence[10] involving threading followed by stoppering (strategy A, Scheme 1) was reversed. Due to the relative

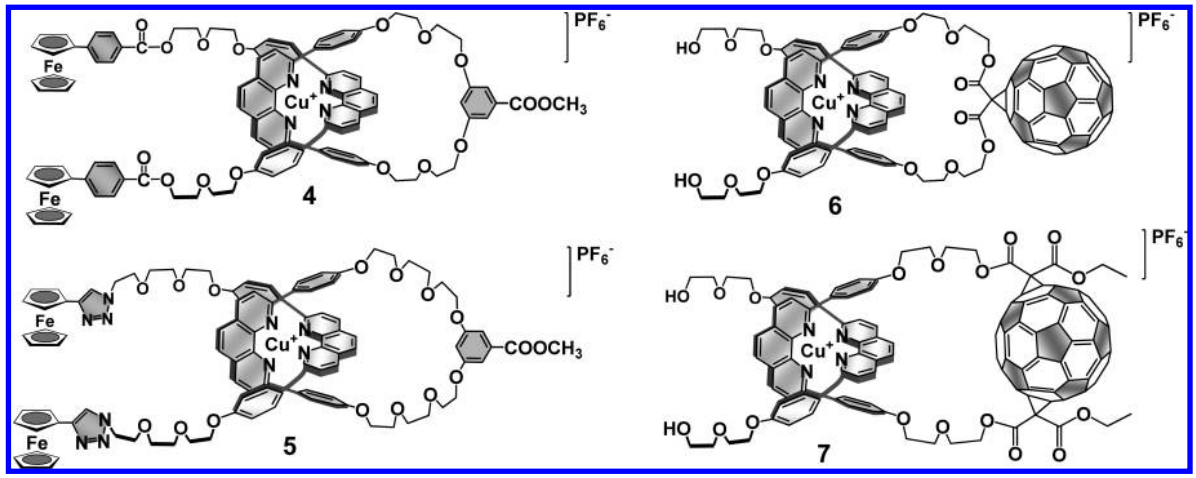

Figure 2. Rotaxane and pseudorotaxane model compounds used for photophysical studies.

SCHEME 1: Representation of the Two Approaches Used To Assemble Rotaxanes in This Work

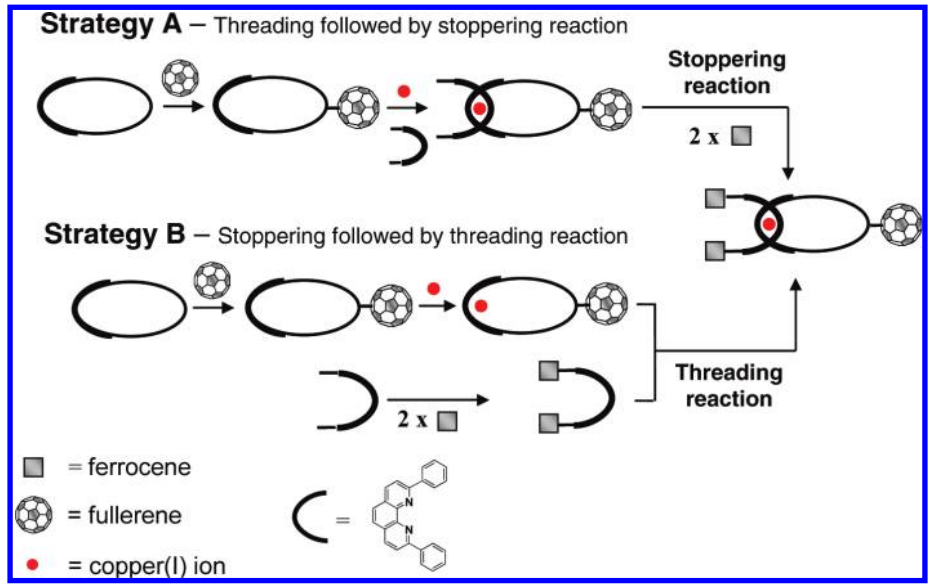

SCHEME 2: Synthetic Strategy and Precursors Used To Prepare Ferrocene-Stoppered Fullerorotaxane 1 and 2[a]

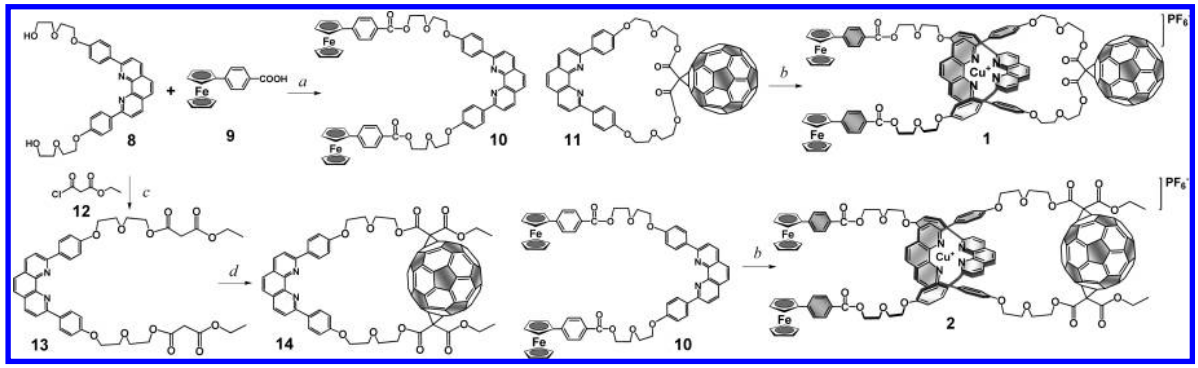

[a] Conditions: (a) DIC/DMAP, CH_2Cl_2, rt, 16 h, 82% yield; (b) $[Cu(CH_3CN)_4][PF_6]$, CH_2Cl_2/CH_3CN, rt, 2 h, 53% yield for **1** and 23% for **2**; (c) DMAP, Et_3N, CH_2Cl_2, 0 °C for 3 h and then rt for 12 h, 85% yield; (d) I_2, C_{60}, DBU, chlorobenzene, rt, 23% yield.

small size of the Fc moiety, we anticipated that a Fc-terminated phen fragment would have no problem threading through the large C_{60}–phen macrocycle precursor. As anticipated, when Fc moieties were first attached to the termini of the phen-containing string, this could be directly threaded through the C_{60}–phen macrocycle using the standard Cu(I) ion template approach to give the target rotaxane.

Fc–C_{60} rotaxane **3** is a more flexible structure in which the length and size of both the macrocycle and thread components were increased by changing the diethylene glycol spacers used in **1** and **2** to triethylene glycol spacers. Because of the higher flexibility of the linker, we anticipated that the direct stoppering–threading approach, strategy B, would probably result in low yields of **3**. Instead, we employed an efficient and straightforward method, which combines the virtues of Cu(I) template synthesis[10] with those of "click" 1,3-dipolar cycloaddition CuAAC chemistry,[13] an approach that has proved to be very effective in our hands for the preparation of highly flexible rotaxanes and catenanes.[14] In this approach, the traditional threading–stoppering sequence of strategy A was adopted in which the Cu(I) ion acts as both template for self-assembly and catalyst for the final "double-click" reactions between ethynylferrocene and a bis-azido-terminated pseudorotaxane, to which C_{60} is already attached, affording rotaxane **3** in very high yields.[14c]

2. Synthesis. The strategy and precursors actually used to prepare rotaxane **1** and **2** are presented in Scheme 2. The route to rotaxane **1** starts with the symmetrical Fc-stoppered thread **10**, which was synthesized in two steps. The ferrocene carboxylic acid **9** was first activated by DIC/DMAP[15] for 10 min at room temperature until a homogeneous orange solution was formed. This activated Fc derivative was then coupled with the phen-diol thread **8**.[10d] The C_{60}–phen macrocycle **11** was prepared by following a published procedure,[9c,14c] while fulleromacrocycle **14** was made by coupling between phen-diol thread **8** and ethyl malonate chloride **12**, followed by attachment of C_{60} using a double Bingel–Hirsch reaction.[16] The ^{1}H NMR spectrum of **14** (see Supporting Information), showed broad peaks,[16a] but nonetheless clearly revealed the absence of the singlet at δ 3.45 ppm assigned to the acidic malonate protons, while the methylene protons of the ester groups appeared at δ 4.50 ppm, in agreement with the structural assignment of **14** as a bis-substituted fullerene adduct. MALDI-TOF analysis confirmed the structure **14**, showing a molecular ion peak at *m*/*z* 1485.9 $(M + H)^+$. Although this procedure is expected to afford a mixture of regioisomeric bis-adducts **14**,[16] the material was used directly in the following steps without further purification.

The usual Cu(I) complexation protocol was then carried out directly using macrocycles **11** and **14** with thread **10**. The threading process was easily monitored by thin layer chromatography (TLC). For example, in the case of rotaxane **1**, TLC initially showed a highly fluorescent spot for macrocycle **11** and a yellow spot corresponding to bis-Fc thread **10**. Complexation of **11** with $[Cu(CH_3CN)_4][PF_6]$ in 3:1 CH_2Cl_2/MeCN

SCHEME 3: Synthetic Strategy and Precursors Used To Prepare the Ferrocene-Stoppered Fullerorotaxane 3[a]

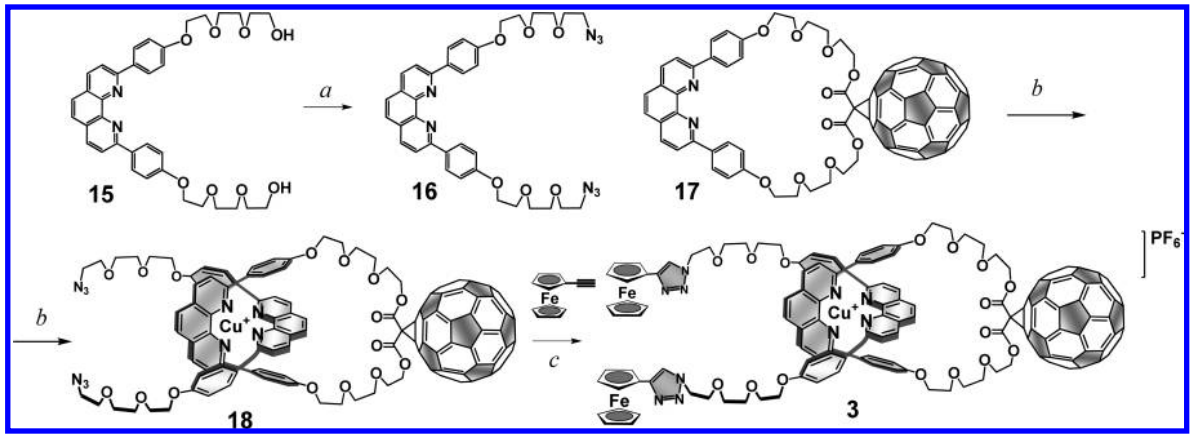

[a] Conditions: (a) (i) TsCl, Et_3N, CH_2Cl_2, 0 °C for 4 h and rt for 20 h, 75% yield; (ii) NaN_3, DMF, 80 °C, 24 h, 93% yield; (b) $[Cu(CH_3CN)_4][PF_6]$, CH_2Cl_2/CH_3CN, rt, 3 h, quantitative; (c) CuI, SA, SBP, DBU, H_2O/EtOH, rt, 12 h, 92% yield.

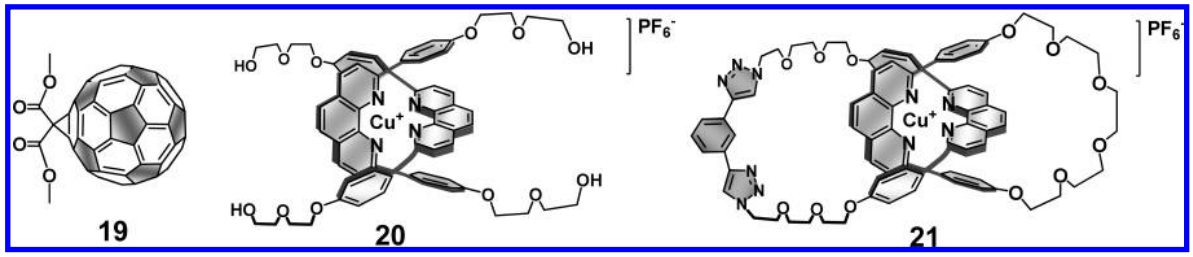

Figure 3. Reference compounds: malonate−C_{60} **19**, (phenanthroline)$_2$−Cu(I) complex **20**, and unsubstituted [2]catenate **21**.

followed by addition of **10** caused disappearance of both these spots, and appearance of a new dark red spot, whose MALDI-TOF mass spectrum corresponded to that of the desired rotaxane **1**, demonstrating that the desired self-assembly process had indeed occurred. The usual workup, followed by chromatographic purification, yielded the target rotaxane **1** in 53% yield. The final product was characterized by ^{1}H NMR and MALDI-TOF spectral analysis (figures not shown; see Supporting Information), which left no doubts as to its structure assignment as a rotaxane. These results confirmed that the cavity of fulleromacrocycle **11** was large enough to allow threading of the bis-Fc-terminated phen string **10** through **11** to occur smoothly under mild conditions. Rotaxanes **2** and **4** were prepared in an analogous manner in 23 and 55% yield, respectively.

The synthesis of 1,2,3-triazole-linked rotaxane **3** by the route shown in Scheme 3 was recently reported elsewhere.[14c] Briefly, threading **16** through macrocycle **17** using the Cu(I) template protocol[10] afforded the fullerene-based pseudorotaxane **18** quantitatively, as revealed by ^{1}H NMR spectroscopy. Finally, two "click" stoppering reactions were accomplished using ethynylferrocene following the conditions reported in our previous communication,[14c] affording rotaxane **3** as a brown amorphous solid in 92% yield. The structure of **3** was confirmed by ^{1}H NMR and MALDI-TOF analysis.[14c] Rotaxane model **5** was prepared in an analogous manner in 95% yield.

3. Electrochemistry. The redox properties of rotaxanes **1**, **2**, and **3**, model compounds **4**, **5**, **6**,[17] and **7**,[17] and the reference compounds shown in Figure 3, namely, C_{60}-malonate-derivative **19**,[13] bis-(phen)$_2$−Cu(I) complex **20**[17] and unsubstituted [2]catenate **21**, were studied by differential and cyclic voltammetry experiments in dichloromethane (DCM) and *o*-dichlorobenzene (ODCB) as solvents in the presence of tetra-*n*-butylammonium hexafluorophosphate ($TBAPF_6$) or tetra-*n*-butylammonium perchlorate ($TBAClO_4$) as supporting electrolyte, with ferrocene/ferrocenium as internal reference. Table 1 shows the electrochemical data obtained at Clemson and Erlangen, respectively.

TABLE 1: Electrochemical Oxidation and Reduction Potentials[a]

	oxidation		reduction			
			$C_{60}/C_{60}^{\bullet-}$			
compound	Fc/Fc^+	Cu^+/Cu^{2+}	$E^{0/-}$	$E^{1-/2-}$	$E^{2-/3-}$	Cu^+/Cu^0
1[b]	+0.048	+0.24	−1.02	−1.42	−1.84	
2[b]	+0.052	+0.25	−1.11	−1.49	−1.92	
3[c]	0	+0.16	−1.04	−1.42	−1.90	−2.30
4[b]	+0.040	+0.24				
5[b]	0	+0.18				−2.30
6[b]		+0.16	−1.01	−1.42	−1.85	−2.30
7[c]		+0.25	−1.11	−1.49	−1.92	
19[b]			−0.99	−1.36	−1.84	
20[c]		+0.16				−2.30
21[c]		+0.16				−2.30

[a] All values (V) are relative to the Fc/Fc^+ internal reference. [b] In dichloromethane and 0.1 M $TBAPF_6$ (Clemson University). [c] In *o*-dichlorobenzene and 0.1 M $TBAClO_4$ (University of Erlangen).

As expected, all rotaxanes display the characteristic redox processes associated with Fc, C_{60}, and $[Cu(phen)_2]^+$ centers. In the case of rotaxanes **1** and **4**, the Fc group exhibits a single, electrochemically reversible two-electron redox wave around 45 mV, corresponding to oxidation of the two Fc groups in the molecule. These Fc groups possess a higher redox potential than does pristine ferrocene, due to the electron withdrawing effect of the nearby carbonyl group. The $[Cu(phen)_2]^+$ complex in **1** and **4** exhibits an one-electron reversible oxidation, which appears in the potential range for this type of derivative.[18] Bis-adduct rotaxanes **2** and pseudorotaxane **7** present similar reduction waves, but these are cathodically shifted with respect to **1** and **4** due to the saturation of a second double bond on C_{60}, causing a negative shift of the reduction potentials.

For the larger more flexible triazole-linked rotaxanes **3** and **5**, three characteristic oxidation features were discernible in the anodic scan. The first process at 0 V was assigned to the one-electron oxidation of Fc, indicating that the introduction of a triazole ring near the Fc group does not have an appreciable electronic effect on the Fc moiety. The second peak at +0.18 V reflects one-electron oxidation of $[Cu(phen)_2]^+$, that is, Cu^+/Cu^{2+}. A third rather broad peak at +1.14 V is tentatively assigned to the Cu^{2+}/Cu^{3+} oxidation (not included in Table 1). In the cathodic scan of **5**, only a single one-electron reduction is seen at −2.30 V, which correlates with the one-electron Cu^+/Cu^0 reduction. In the case of 3, one sees in addition the typical values associated with C_{60} reduction.[19]

Comparison of the electrochemical data of the rotaxanes with their model compounds, conducted under the same experimental conditions, reveals that the presence of the C_{60} moiety in the molecule has no noticeable impact on the oxidation and reduction potentials of the other components. These results demonstrate that the various constituents do not electronically couple or strongly interact with each other in the ground state.

4. Steady-State and Time-Resolved Fluorescence Studies. Fluorescence experiments provided initial insights into the photoinduced processes occurring in the new rotaxanes. Figure 4 shows the fluorescence spectra of several rotaxanes as well as those of the corresponding reference compounds, while Table 2 summarizes the spectroscopic data collected for all compounds studied.

The data for $[Cu(phen)_2]^+$ complex **20** and unsubstituted [2]catenate **21** will be discussed first. Both **20** and **21** exhibit emission centered at 765 nm, with quantum yields of 3.0×10^{-4} and 4.8×10^{-3}, respectively, and identical fluorescence lifetimes of 2.5 ns in benzonitrile (PhCN). This emission of **21** originates from deactivation of the thermally equilibrated singlet and triplet MLCT excited states of the $[Cu(phen)_2]^+$ complex. We note that the fluorescence quantum yield for the more flexible structure **20** is lower than that for the more rigid structure **21**, as expected.

The luminescence properties of rotaxane **1** reflect the interchromophoric interactions in these systems upon photoexcitation. Quenching of the MLCT-type emission band of the $[Cu(phen)_2]^+$ moiety is evident (Figure 4A). The luminescence quantum yields and lifetimes of rotaxanes **1** and **2** in PhCN, namely 6.8×10^{-6}/40 ps and 1.2×10^{-5}/77 ps, respectively, are much lower than those of the model compounds **20**, **21**, and **4**. This indicates that additional photophysical pathways are at work in **1** and **2**. It is important to note that the quantum yields for **1** and **2** are very close to those for pseudorotaxanes **6** (3.8×10^{-5}) and **7** (1.3×10^{-5}). Quenching of the electronically excited $[Cu(phen)_2]^+$ moiety in **1** and **2** located 1.70 eV above the ground state is attributed to highly efficient electron transfer to C_{60} from the lowest MLCT state, to give the energetically lower lying radical ion pair $[Cu(phen)_2]^{2+}-C_{60}^{\bullet-}$ located at 1.33 eV, as estimated from the electrochemical data in Table 1.

Turning now to the more flexible triazole-linked structures, excitation of $[Cu(phen)_2]^+-Fc_2$ model rotaxane **5** at 320 nm produces a rather broad emission band centered at 765 nm (see Figure 4B), attributed to luminescence from the MLCT excited state of $[Cu(phen)_2]^+$. The quantum yield is 6×10^{-4} in DCM or ODCB and 1.6×10^{-3} in PhCN, lower than those measured for **20** and **21** but higher than that measured for $[Cu(phen)_2]^+-C_{60}$ pseudorotaxane **6**. Upon 355 nm excitation of C_{60} in $Fc_2-[Cu(phen)_2]^+-C_{60}$ rotaxane **3**, we observe moderate quenching of the C_{60} emission (see Figure 4c). In PhCN, the fluorescence quantum yield is reduced to 2×10^{-4} compared to 6×10^{-4} for the C_{60} reference **19**. Considering the fact that energy transfer from the weakly fluorescing C_{60} singlet excited state (1.78 eV) to the $[Cu(phen)_2]^+$ singlet excited state (1.92 eV) is thermodynamically unfavorable, charge transfer is left as the only feasible deactivation pathway for **3**. The fluorescence quenching seen in Figure 4C was corroborated by time-resolved fluorescence measurements. The fluorescence lifetime of 0.1 ns for rotaxane **3** is much lower than 1.4 ns observed for C_{60} reference compound **19**. These data for **3**

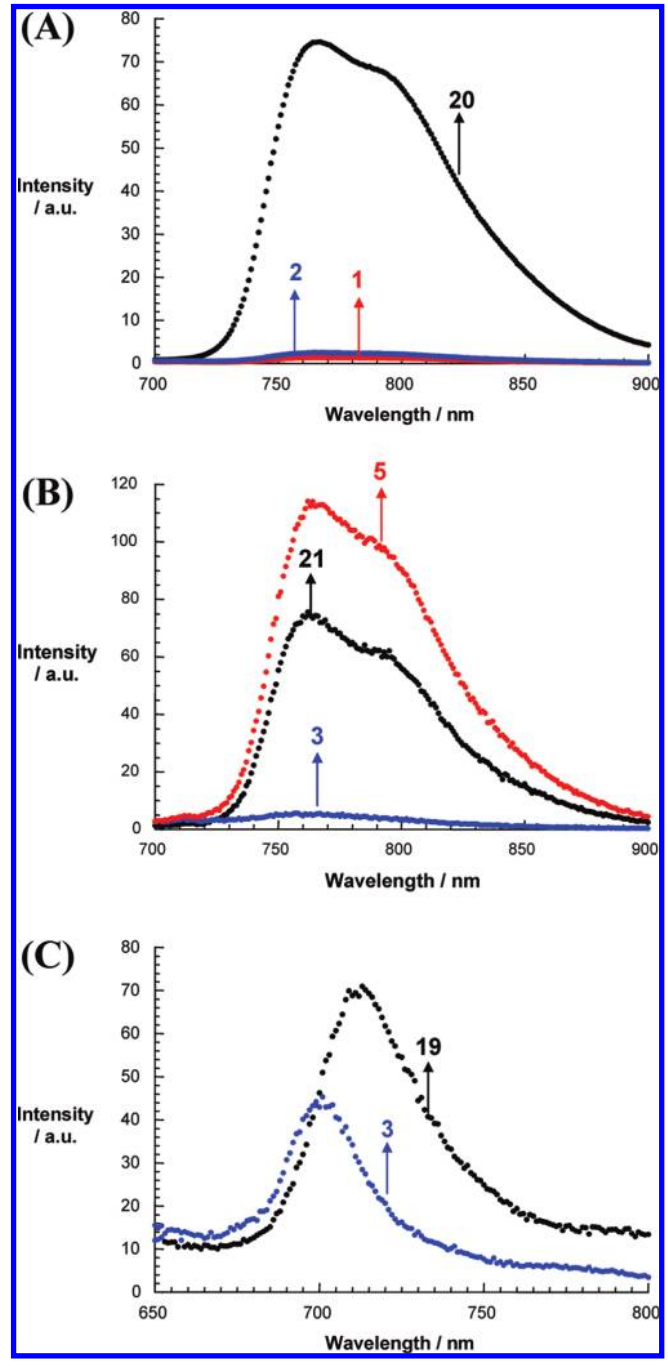

Figure 4. Fluorescence spectra at room temperature in benzonitrile. (A) Rotaxanes **1** and **2**, and (phenanthroline)$_2$−Cu(I) complex **20** using solutions having the same optical density (0.25) at the excitation wavelength of 320 nm. (B) Rotaxanes **3**, **5**, and model [2]catenate **21** using solutions having the same optical density (0.15) at the 320 nm excitation wavelength. (C) Rotaxane **3** and C_{60}-reference **19** using solutions having optical density 0.4 at the 355 nm excitation wavelength.

TABLE 2: Fluorescence Parameters and Charge Separated State Lifetimes at 298 K in Air-Equilibrated Solutions[a]

compound	excited state	λ_{max} (nm)	τ_{lum} (ns)	Φ_F	τ_{CR} (ns)
1[b]	Fc−*Cu$^+$−C_{60}	765	0.04	6.8×10^{-6}	16
2[b]	Fc−*Cu$^+$−C_{60}	765	0.08	1.2×10^{-5}	16
3[b]	Fc−Cu$^+$−C_{60}*	700	0.10	2.0×10^{-4}	15
5[b]	Fc−*Cu$^+$	765	2.0	1.6×10^{-3}	
7[b]	*Cu$^+$−C_{60}	765		1.3×10^{-5}	16
19[c]	$^1C_{60}$*	920	1.4	6.0×10^{-4}	
	$^3C_{60}$*	700[d]	2.0×10^4		
20[e]	MLCT[1]	765	5.2	3×10^{-4}	
21[b]	MLCT	765	2.5	4.8×10^{-3}	

[a] λ_{max} = maxima emission; τ_{lum} = fluorescence lifetime; Φ_F = fluorescence quantum yield; τ_{CR} = lifetime of the charge separated state. [b] In benzonitrile. [c] In *o*-dichlorobenzene. [d] From ref 19. [e] From ref 9a.

should be compared with those of [Cu(phen)$_2$]$^+$−C_{60} pseudorotaxane **6** (figure not shown) in which the C_{60} fluorescence quantum yield under these conditions is reduced to 2.3×10^{-5} in PhCN. The fluorescence quenching observed for both **3** and **6** is attributed to ET from the Cu(I) complex to C_{60} (*vide infra*). These data are summarized in Table 2.

5. Transient Absorption Studies. Further insight into the formation and decay processes of the photoexcited rotaxanes was obtained by transient absorption studies in PhCN. Excitation of C_{60} reference compound **19** at 387 nm (figure not shown) populates the fullerene singlet excited state with characteristic absorption maxima at 610 and 920 nm.[19] The latter undergoes quantitative intersystem crossing to the triplet manifold with a characteristic lifetime of 1.4 ns.[19] In the absence of molecular oxygen, the C_{60} triplet excited state ($^3C_{60}$*) has a lifetime of up to 20 μs.

Photoexcitation of the [Cu(phen)$_2$]$^+$ complex **20** and unsubstituted [2]-catenate **21** at 387 nm in an oxygen free environment generates MLCT excited states. The intermediate singlet MLCT excited state is discernible immediately following the excitation of **20**, for which a transient maximum is seen at 490 nm, which decays with a lifetime of 0.43 ps[20] to form the triplet MLCT excited state, which has maxima at 540 and 1000 nm (see Figure 5). Additional minima evolve in the 440 and 700 nm regions, which correspond well with the MLCT absorption and attest to conversion of the ground state into the corresponding MLCT excited state. On the 3 ns time scale of the femtosecond experiments, no appreciable decay of the triplet MLCT excited state is seen. Upon nanosecond excitation of **20** at 355 nm similar characteristics develop, with a lifetime of 886 ns in deaerated PhCN, assigned to the phenanthroline triplet excited state formed by an energy transfer process.[21]

Excitation at 387 nm of (Fc)$_2$−[Cu(phen)$_2$]$^+$ rotaxanes **4** and **5**, lacking the C_{60} moiety, generated the MLCT excited states of [Cu(phen)$_2$]$^+$ with characteristic absorption maxima at 590 nm and a broad absorption centered around 880 nm (see Figure 6 for spectra of rotaxane **5**). Again, the MLCT triplet excited state of **5** is long-lived and does not decay appreciably on the time scale of our femtosecond laser experiments (i.e., up to 3 ns). It is clear that, on this time scale, Fc does not exert any notable impact on the triplet [Cu(phen)$_2$]$^+$ MLCT excited state of **5**.

In (Fc)$_2$−[Cu(phen)$_2$]$^+$−C_{60} rotaxane **3**, 387 nm excitation is mainly directed to the C_{60} unit due to its dominant absorption in that spectral region.[19] Instantaneous growth of absorption at 900 nm confirms generation of $^1C_{60}$*, which decays with accelerated dynamics, attributable to the nearby [Cu(phen)$_2$]$^+$ subunit (see Figure 7). The average of the first-order fits of the time−absorption profiles at various wavelengths gives a value of only 35 ps for the $^1C_{60}$* lifetime in **3**, which matches the strongly quenched $^1C_{60}$* emission (see above). As the C_{60} singlet excited state decays, new transients evolve with broad absorption in the visible region centered at 590 nm, the signature of [Cu(phen)$_2$]$^{2+}$. At the same time, some new absorption rapidly evolves in the near-infrared region with a maximum at 1035 nm, which is the well-documented fingerprint absorption of the one-electron reduced form of C_{60}, i.e., $C_{60}^{\bullet-}$.[19] Thus, the transient absorption studies confirm the formation by electron transfer (ET) of the radical ion pair (Fc)$_2$−[Cu(phen)$_2$]$^{2+}$−$C_{60}^{\bullet-}$, which is stable on the picosecond time scale. Additionally, we see spectroscopic evidence in the visible region for the formation of the singlet MLCT excited state (λ_{max} 490 nm), which is transformed with lifetimes of 0.43 and 14 ps into the triplet MLCT excited state (λ_{max} 530 nm) and the radical ion pair state (λ_{max} 590 nm), respectively.

In complementary nanosecond experiments, excitation of triazole-linked rotaxane **3** at 355 nm in PhCN leads to the same radical ion pair spectral features characteristic of $C_{60}^{\bullet-}$ and [Cu(phen)$_2$]$^{2+}$ (figure not shown). A multiwavelength analysis for decay of the transient absorption revealed two major decay components for (Fc)$_2$−[Cu(phen)$_2$]$^{2+}$−$C_{60}^{\bullet-}$, a short-lived oxy-

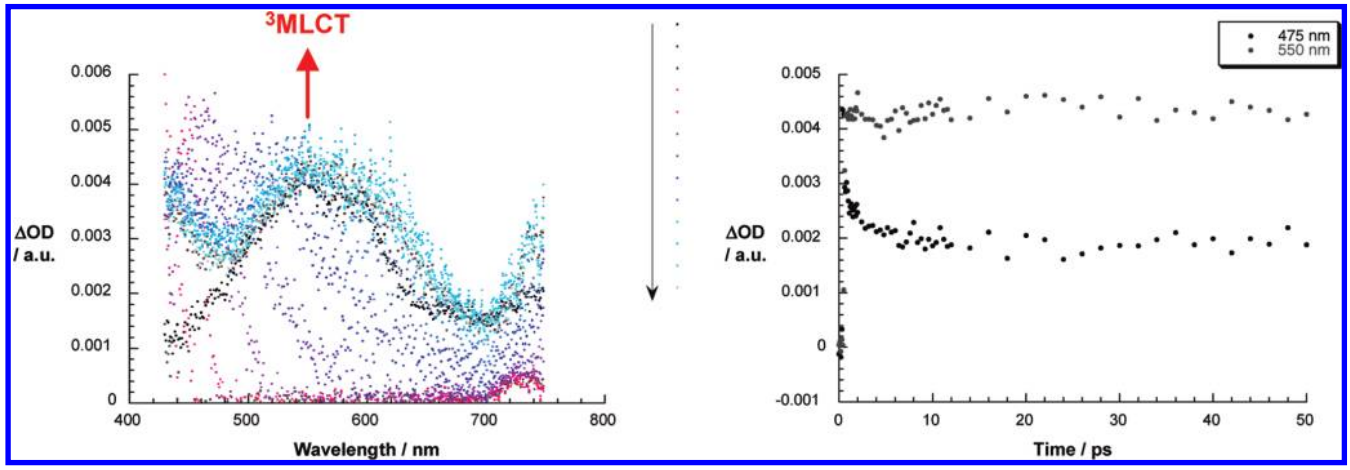

Figure 5. Left: differential absorption spectra (i.e., visible and near-infrared) obtained upon femtosecond flash photolysis (387 nm) of [Cu(phen)$_2$]$^+$ complex **20** in benzonitrile with time delays between 0 and 10 ps at room temperature (see figure legend/arrow for details of time progression). Right: time−absorption profiles at 475 and 550 nm of the spectra on the left reflecting the excited state dynamics.

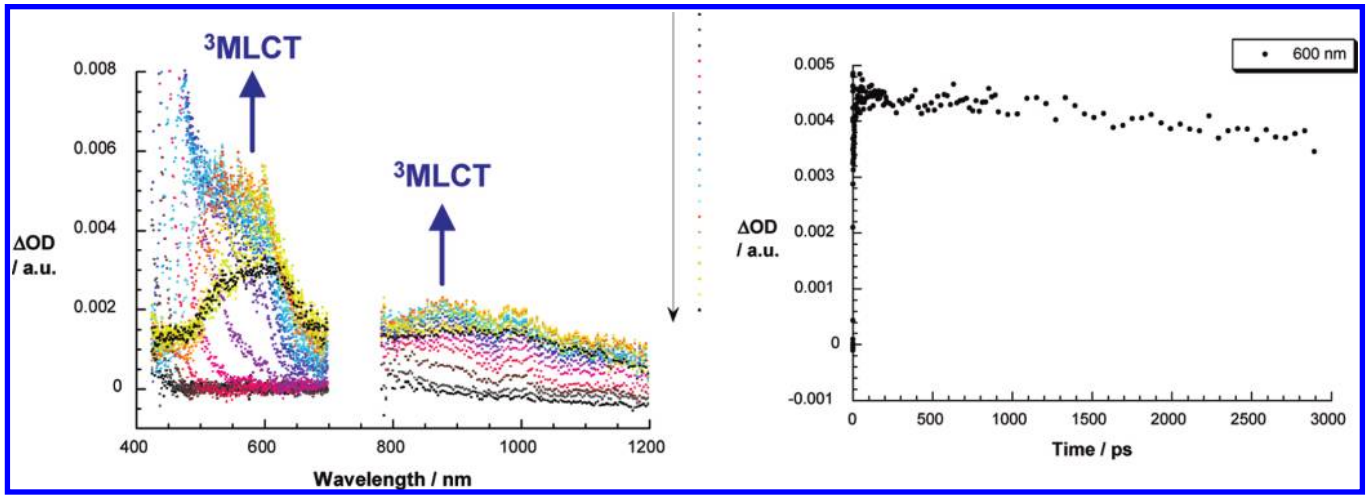

Figure 6. Left: differential absorption spectra (i.e., visible and near-infrared) obtained upon femtosecond flash photolysis (387 nm) of $(Fc)_2-[Cu(phen)_2]^+$ rotaxane **5** in benzonitrile with time delays between 0 and 200 ps at room temperature (see figure legend/arrow for details of time progression). Right: time−absorption profiles at 600 nm of the spectra on the left reflecting the excited state dynamics.

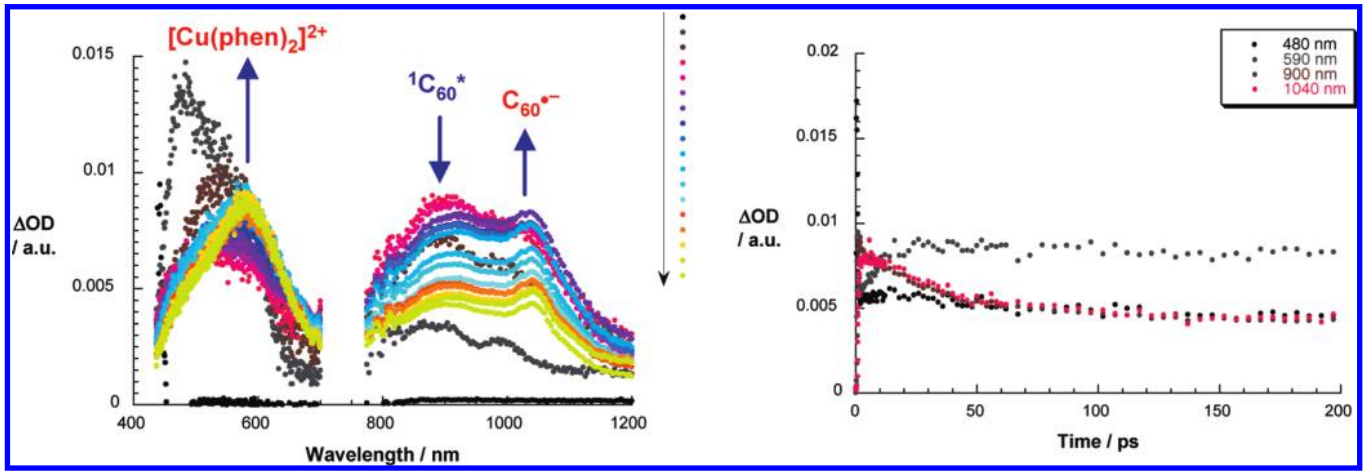

Figure 7. Left: differential absorption spectra (i.e., visible and near-infrared) obtained upon femtosecond flash photolysis (387 nm) of rotaxane **3** in benzonitrile with different time delays between 0 and 100 ps at room temperature (see figure legend/arrow for details of the time progression). Right: time−absorption profiles at 480, 590, 900, and 1040 nm of the spectra on the left reflecting the charge-separation dynamics.

gen concentration-independent component and a long-lived oxygen dependent component. We believe that the short-lived component, decay time 15 ns, corresponds to charge recombination to afford the singlet ground state. Independent confirmation for this conclusion comes from a freshly prepared sample of pseudorotaxane **6**,[17] which lacks the Fc units, whose radical ion pair state also decays with a lifetime of 15 ns. A possible rationale for the second component whose lifetime is 121 ns emerges upon consideration of the driving force of −0.16 eV for a charge shift process, i.e., movement of the positive charge from the $[Cu(phen)_2]^{2+}$ complex to Fc to give $(Fc)_2^{\bullet+}-[Cu(phen)_2]^+-C_{60}^{\bullet-}$. We estimate the energies of the two charge-separated states as 1.20 and 1.04 eV, respectively, on the basis of our electrochemical data (Table 1).[22] Once again, the low extinction coefficient of one-electron oxidized Fc even at its maximum absorption of 680 nm[12] renders this spectroscopic identification uncertain, however plausible. Direct forward and back ET between Fc and C_{60} is not likely due to the large donor−acceptor separation, close to 2 nm. Accordingly, we anticipated that the lifetime of the long distance radical ion pair state of **3**, $(Fc)_2^{\bullet+}-[Cu(phen)_2]^+-C_{60}^{\bullet-}$, would be at least 1 μs, as seen in the covalent systems described previously in which ET from Fc to other oxidized species was invoked.[12] This was not observed in our experiments.[23,24] To shed further light on this issue, experiments were carried out at different oxygen concentrations, that is, in oxygen-saturated, air-saturated, and argon-saturated solutions. It is noteworthy that the short-lived decay component of 15 ns remains constant throughout these measurements, while the lifetime of the longer-lived component varies between 121 ns and 7.7 μs. The resemblance of the latter response to quenching of C_{60} triplet excited states by molecular oxygen[19] forces us to conclude that the longer-lived component is in fact the triplet excited state C_{60} rather than the $(Fc)_2^{\bullet+}-[Cu(phen)_2]^+-C_{60}^{\bullet-}$ radical ion pair state. Nevertheless, we cannot absolutely rule out the possible generation of this long distance CS state as long as it has a lifetime as short as 121 ns. On the basis of the driving forces for charge recombination (−1.2 eV) and charge shift (−0.16 eV), in the initially generated CS state of **3**, along with a reorganization energy of ~0.8 eV,[19b] it is clear that the former process (i.e., charge recombination) should be in the Marcus inverted region, while the latter (i.e., charge shift) should be in the normal region of the Marcus parabola. Correspondingly, we estimate—assuming similar electronic couplings—that the charge shift reaction is three orders of magnitude slower than charge recombination. We estimate that the efficiency of the second charge shift in this case, from Fc to the oxidized Cu complex, is at most 0.001%.

Similarly, in studies of **1** (Figure 8) and **2** (Figure 9), we note that instead of the slow intersystem crossing dynamics, the singlet−singlet absorption of C_{60} (i.e., at 900 and 920 nm) decays

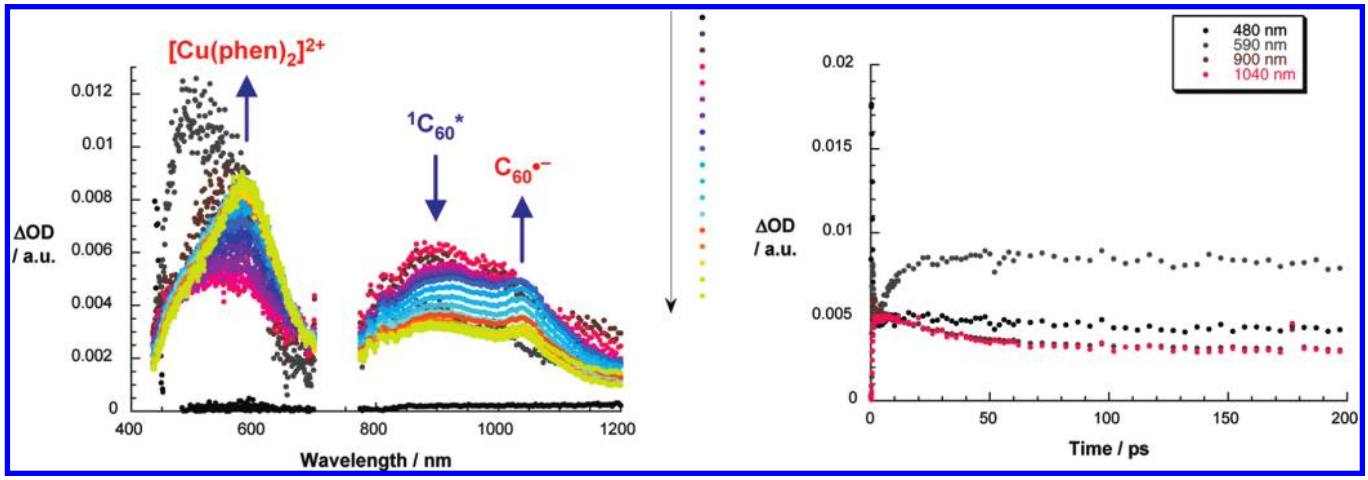

Figure 8. Left: differential absorption spectra (i.e., visible and near-infrared) obtained upon femtosecond flash photolysis (387 nm) of rotaxane **1** in benzonitrile with different time delays between 0 and 200 ps at room temperature (see figure legend/arrow for details of time progression). Right: time−absorption profiles at 480, 590, 900, and 1040 nm of the spectra on the left reflecting the charge-separation dynamics.

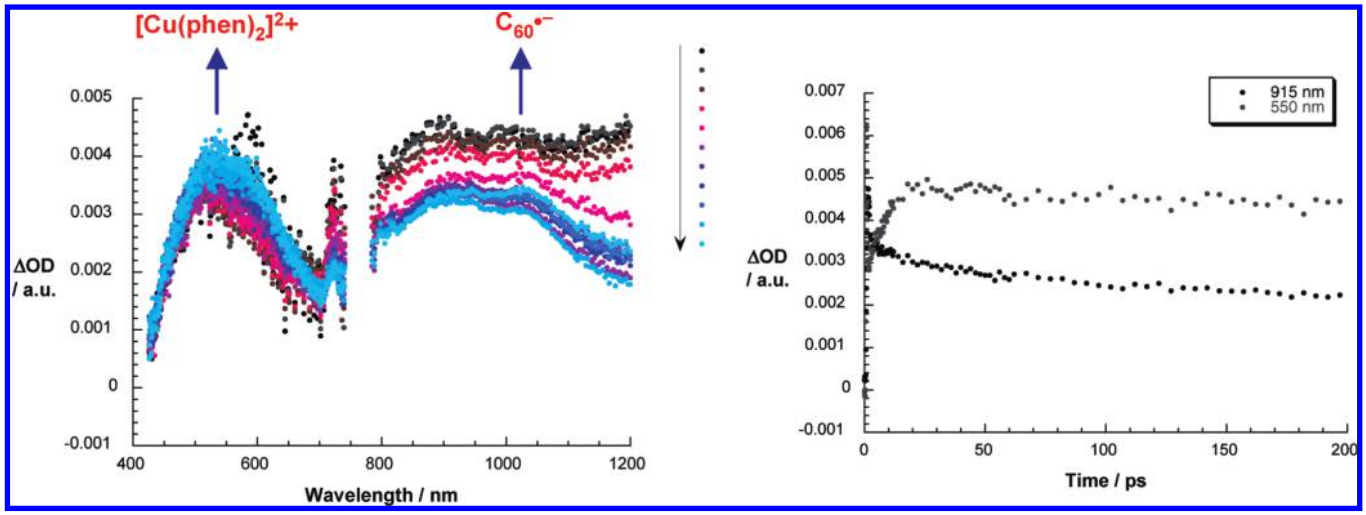

Figure 9. Left: differential absorption spectra (i.e., visible and near-infrared) obtained upon femtosecond flash photolysis (387 nm) of **2** in benzonitrile with different time delays between 0 and 200 ps at room temperature (see figure legend/arrow for details of time progression). Right: time−absorption profiles at 550 and 915 nm of the spectra on the left reflecting the charge-separation dynamics.

in the presence of $[Cu(phen)_2]^+$ complex with accelerated dynamics, along with the enhanced decay of the rapidly formed (i.e., 0.43 ps) triplet MLCT excited state (i.e., at 540 nm). There is a close resemblance of the dynamics noted in **1** (lifetimes 33 and 9 ps) and **2** (48 and 15 ps) with those in **3** (35 and 14 ps). In all three cases, new transients are seen in the visible range, which match those of the one-electron oxidized $[Cu(phen)_2]^{2+}$ at 590 nm, and, in the near-infrared, the one-electron reduced $C_{60}^{\bullet-}$ at 1035 nm. Thus, the spectroscopic features of the observed transients confirm the formation of a radical ion pair state, which is stable on the femtosecond and picosecond time scales.

We examined the charge-recombination dynamics for first generation $C_{60}-(Fc)_2$ ester-linked rotaxanes **1** and **2** on the nanosecond time scale in PhCN using 6 ns laser pulse excitation at 355 nm. In this context, the spectral fingerprints of the radical ion pair state, $Fc_2-[Cu(phen)_2]^{2+}-C_{60}^{\bullet-}$ are seen immediately after the nanosecond laser pulse, indicating these states are the ultimate product of the charge transfer process.[19] The lifetime of the CS states of both **1** and **2** is 16 ns, determined by the decay of the fingerprint absorption for $C_{60}^{\bullet-}$ at 1035 nm. Quite interestingly, these values of 16 ns exactly match the CS state lifetimes determined for pseudorotaxane reference compounds **6** and **7** lacking Fc moieties as well as the lifetime of 15 ns determined for the triazole linked $C_{60}-(Fc)_2$ rotaxane **3**. The small molar extinction coefficient of the ferrocenium ion at 800 nm unfortunately precludes direct detection of the formation and decay of $Fc^{\bullet+}$.[12] The quite short lifetime of the charge separated states in these rotaxanes, on the order of 16 ns, argues against the proposal that $Fc_2^{\bullet+}-[Cu(phen)_2]^+-C_{60}^{\bullet-}$ charge separated radical ion pair states are formed in rotaxanes **1**−**3**, contrary to the claim in the recent paper of Ito and coworkers on Al(III) porphyrin−C_{60}−Fc triads.[23] In addition to the short-lived CS states detected in rotaxanes **1**−**3**, a longer-lived component is observed, whose lifetime depends strongly on the oxygen concentration. Thus, while lifetimes of 126 and 115 ns are observed for **1** and **2**, respectively, in oxygen-saturated PhCN, much longer lifetimes are observed in oxygen-free solutions. While we cannot unambiguously exclude the possibility that these values represent upper limits for the lifetimes of $(Fc)^{\bullet+}-[Cu(phen)_2]^+-C_{60}^{\bullet-}$ radical ion pair states, we consider it much more likely that they are due to C_{60} triplet excited states formed by intersystem crossing from $^1C_{60}$* in competition with charge separation following excitation of rotaxanes **1** and **2**, as shown in Figure 10.

Conclusions

On the basis of our findings, we propose the energy level diagram and decay pathways shown in Figure 10 for rotaxanes

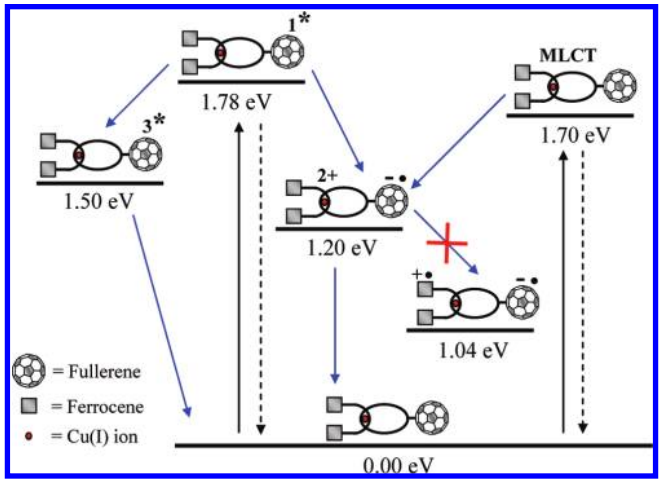

Figure 10. The energy values in the Figure for the charge separated states are for rotaxane **3** in ODCB as determined from electrochemical measurements.

1, **2**, and **3** upon excitation of either the $[Cu(phen)_2]^+$ or C_{60} moieties. In all three cases, excitation at 387 nm induces an electron transfer (ET) process to give the charge separated state $(Fc)_2-[Cu(phen)_2]^{2+}-C_{60}^{\bullet-}$, with an oxidized $Cu(phen)_2$ complex and a reduced C_{60}. This charge separated state has a lifetime of 15−16 ns in benzonitrile, virtually identical to model compounds lacking ferrocene moieties. Thus, a charge shift from the Fc moiety to the $[Cu(phen)_2]^{2+}$ to generate a long-distance CS state does not appear to take place in these rotaxanes. This conclusion is based mainly on the lack of elongation of the CS state lifetime on introducing Fc moieties into the system, despite the fact that such a charge shift process is predicted to be exergonic by 0.16 to 0.20 eV. It certainly would be advantageous to be able to follow the formation and decay of $Fc^{\bullet+}$ moieties to absolutely confirm this conclusion, but to date this has not proved possible. These findings are in contrast to previous reports on the photophysics of covalently linked donor−acceptor triads and related $Fc-ZnP-H_2P-C_{60}$ tetrads in which the CS lifetime is significantly elongated by introducing Fc groups, an effect attributed to a charge shift from the $ZnP^{\bullet+}$ to the Fc moieties,[12] as well as the recent report on an $Al(III)-C_{60}-Fc$ triad mentioned earlier.[23] In rotaxanes **1**−**3**, ET from Fc to the oxidized $[Cu(phen)_2]^{2+}$ complex to generate the analogous long-distance CSRP state $^{\bullet+}(Fc)_2-[Cu(phen)_2]^{+}-C_{60}^{\bullet-}$ does not appear to be competitive with charge recombination from the initially formed CS state to regenerate the electronic ground state of the rotaxane. This could be due to the increased dimensions of the rotaxanes, in which the center-to-center distance between the Fc stoppers and $[Cu(phen)_2]^+$ cores is 1.0 nm in rotaxane **1** and further increases to 1.8−1.9 nm of rotaxane **3**, both in extended conformations. For the covalent systems,[12] linkage is provided by an amide group and the Fc−ZnP distance is also much shorter. However, it is worthy of note that in triazole-linked rotaxanes analogous to **3** with ZnP stoppers in place of Fc and identical dimensions, photoinduced electron transfer does take place to give the long-lived long distance charge separated radical pair state $(ZnP)_2^{\bullet+}-[Cu(phen)_2]^{+}-C_{60}^{\bullet-}$. Details of this investigation will be reported shortly.[24] Obviously, in rotaxane systems with similar dimensions, electronic coupling between ZnP and the oxidized $[Cu(phen)_2]^{2+}$ complex is much better than coupling between Fc and the identical Cu^{2+} complex.

Experimental Section

1. General Information and Materials. NMR spectra were obtained on either a Bruker AVANCE 400 (400 MHz) or an AVANCE 500 (500 MHz) spectrometer using deuterated solvents as the lock. The spectra were collected at 25 °C, and chemical shifts (δ, ppm) were referenced to the residual solvent peak (^1H, $CDCl_3$ at 7.26 ppm; ^{13}C at 77.2 ppm). In the assignments, the chemical shift (in ppm) is given first, followed, in brackets, by multiplicity (s, singlet; d, doublet; t, triplet; m, multiplet; br, broad), the value of the coupling constants in hertz if applicable, the number of protons implied, and finally the assignment. In the ^1H NMR assignment (δ), H_o and H_m refer to the hydrogen atoms at the ortho and meta positions, respectively, of the phenyl ring attached to the phenanthroline ring system, whose hydrogen atoms are numbered $H_{3,8}$, $H_{4,7}$, $H_{5,6}$, respectively. Ar and Cp are used as abbreviations for aromatic and cyclopenadienyl rings, respectively. Mass spectra were obtained on an Agilent 1100 Series Capillary LCMSD Trap XCT spectrometer in positive or negative-ion mode and ThermoFinnigan PolarisQ ion-trap GCMS spectrometer. MALDI-TOF mass spectra were recorded in a Bruker OmniFLEX MALDI-TOF MS spectrometer. This instrument was operated at an accelerating potential of 20 kV in linear mode. The mass spectra represent an average over 256 consecutive laser shots. The mass scale was calibrated using the matrix peaks and the calibration software available from Bruker OmniFLEX. Mentioned *m*/*z* values correspond to monoisotopic masses. The compound solutions (10^{-3} mol/L) were prepared in THF. The matrix compound was purchased from Aldrich and used without further purification. The matrix, α-cyano-4-hydroxycinnamic acid (CCA), was dissolved (10 g/L) in a solvent mixture composed of water/acetonitrile/trifluoroacetic acid (25/75/1, v/v). Two microliters of compound solution were mixed with 10 μL of matrix solution. The final solution was deposited onto the sample target and allowed to dry in air. All chemicals were purchased from Sigma-Aldrich and Alfa Aesar and used without further purification. For moisture sensitive reactions, solvents were freshly distilled. Methylene chloride (DCM), toluene (PhMe), and acetonitrile (CH_3CN) were dried over calcium hydride while tetrahydrofuran (THF) was dried using sodium/benzophenone. Anhydrous dimethylformamide (DMF) was used as received. All syntheses were carried out using Schlenk line techniques. Moisture sensitive liquids were transferred by canula or syringe. The progress of the reactions was monitored by thin-layer chromatography (TLC) whenever possible. TLC was performed using precoated glass plates (Silica gel 60, 0.25 mm thickness) containing a 254 nm fluorescent indicator. Column chromatography was carried out using Merck Silica gel 60 (0.063−0.200 mm). Compounds **8**,[10d] **11**,[9,14c] **15**,[10d] **16**,[14c] and **17**[14c] were synthesized following literature procedures.

2. Electrochemical Studies. The solution electrochemistry of compounds **1**−**7** and reference systems **19**−**21** was investigated by cyclic voltammetry (CV) and Osteryoung square wave voltammetry (OSWV). The solutions were prepared at concentrations between 0.1−0.5 mM in deoxygenated methylene dichloride (CH_2C_{l2}) or *o*-dichlorobenzene (*o*-DCB), and containing tetra-*n*-butylammonium hexafluorophosphate (TBAPF6) (0.1 M) or tetra-*n*-butylammonium perchlorate ($TBAClO_4$) as supporting electrolytes, respectively. A glassy carbon electrode (3 mm diameter) was used as the working electrode, a platinum mesh as the counter, and $Ag/AgNO_3$ (CH_3CN) as reference electrode. Ferrocene was added as an internal reference and all values are reported vs ferrocene. For derivatives **1**, **2**, **4**, and **6** (see Figures 1 and 2) decamethylferrocene was added as an

internal reference and it was referenced against ferrocene. The redox potentials are summarized in Table 1.

All electrochemical measurements were performed with a BAS 100 W electrochemical analyzer (Bioanalytical systems) or an EGC Princenton Applied Research model 263A potentiostat/galvanostat.

3. Photophysical Studies. Femtosecond transient absorption studies were performed with 387 and 420 nm laser pulses (1 kHz, 150 fs pulse width) from an amplified Ti:sapphire laser system (Model CPA 2101, Clark-MXR Inc.). Nanosecond laser flash photolysis experiments were performed with 355 or 532 nm laser pulses from a Quanta-Ray CDR Nd:YAG system (6 ns pulse width) in front face excitation geometry. Fluorescence lifetimes were measured by using a Fluorolog (Horiba Jobin Yvon). Steady-state fluorescence measurements were performed by using a Fluoromax 3 (Horiba Jobin Yvon). The experiments were performed at room temperature.

4. Synthesis. ***Thread Compound 10.*** 1,3-Diisopropylcarbodiimide (DIC) (0.150 g, 1.20 mmol) was added to a suspension of *p*-ferrocenylbenzoic acid **9** (0.320 g, 1.05 mmol) and 4-(dimethylamino)pyridine (DMAP) (0.050 g, 0.41 mmol) in dry CH_2Cl_2 (10 mL) at room temperature. The suspension turned into orange solution quickly. After 15 min, phen-diol **12** (0.270 g, 0.50 mmol) was added to the orange solution as a solid and the mixture was stirred for 16 h. The precipitated *N*,*N*′-diisopropylcarbourea was removed by filtration and the filtrate was subject to column chromatography (SiO_2) using CH_2Cl_2/CH_3OH (98:2, v/v) to afford **10** as a orange powder in 82% yield (0.46 g).^{1}H NMR ($CDCl_3$), δ, ppm: 8.44 (d, J = 8.8 Hz, 4H, $\underline{H}_o$); 8.24 (d, J = 8.5 Hz, 2H, $\underline{H}_4$ and $\underline{H}_7$); 8.07 (d, J = 8.5 Hz, 2H, $\underline{H}_3$ and $\underline{H}_8$); 7.96 (d, J = 8.3 Hz, 4H, ferrocene ortho Ar-$\underline{H}$); 7.73 (s, 2H, $\underline{H}_5$ and $\underline{H}_6$); 7.46 (d, J = 8.3 Hz, 4H, ferrocene meta Ar-$\underline{H}$); 7.22 (d, J = 8.8 Hz, 4H, $\underline{H}_m$); 4.65 (t, J = 4.9 Hz, 4H, Ar−COO-C$\underline{H}_2$); 4.52 (t, J = 4.9 Hz, 4H, C$\underline{H}_2$−O−phenanthroline); 4.30−3.90 (m, 26H, O−C$\underline{H}_2$−C$\underline{H}_2$−O and Cp-$\underline{H}$); MALDI-TOF: *m*/*z* found 1116.94 $[M + H]^+$, calculated 1116.27 for $C_{66}H_{56}N_2O_8Fe_2$.

Compound 13. Diol **8** (1.08 g, 2.0 mmol) was dissolved in dry (50 mL) CH_2Cl_2. The solution was cooled to 0 °C in an ice bath; then Et_3N (1.0 mL) and DMAP (0.005 g, 0,041 mmol) were added. The subsequent addition of ethylmalonyl chloride **12** (0.60 g, 4 mmol) was made by syringe dropwise. The solution was then allowed to stir at 0 °C for 3 h, and then at room temperature (rt) for 12 h. TLC indicated that the reaction had proceeded to completion. The reaction mixture was extracted with HCl (5%) and then saturated $NaHCO_3$ solutions. The organic layer was washed with water (150 mL), dried over $MgSO_4$, filtered through paper, and concentrated under reduced pressure. The resulting oil residue was subjected to column chromatography (SiO_2) using CH_2Cl_2/CH_3OH (98:2, v/v) to afford **13** as a yellow oil in 85% yield (1.30 g). ^{1}H NMR ($CDCl_3$), δ, ppm: 8.43 (d, J = 8.8 Hz, 4H, $\underline{H}_o$); 8.25 (d, J = 8.5 Hz, 2H, $\underline{H}_4$ and $\underline{H}_7$); 8.05 (d, J = 8.5 Hz, 2H, $\underline{H}_3$ and $\underline{H}_8$); 7.73 (s, 2H, $\underline{H}_5$ and $\underline{H}_6$); 7.08 (d, J = 8.8 Hz, 4H, $\underline{H}_m$); 4.38 (t, 4H, COO−C$\underline{H}_2$−CH_3); 4.25 (t, J = 4.9 Hz, 4H, C$\underline{H}_2$−O−phenanthroline); 4.20−3.80 (m, 12H, O−C$\underline{H}_2$−C$\underline{H}_2$−O); 3.45 (s, 4H, O=C−C$\underline{H}_2$−C=O); 1.25 (s, 6H, O−CH_2−C$\underline{H}_3$). LCMS: *m*/*z* found 769.1 $[M + H]^+$, calculated 768.3 for $C_{42}H_{44}N_2O_{12}$.

Macrocycle 14. Phen dimalonate **13** (0.153 g, 0.20 mmol), C_{60} (0.144 g, 0.2 mmol), and I_2 (0.107 g, 0.42 mmol) were dissolved in dry chlorobenzene (80 mL) under a N_2 atmosphere. 1,8-Diazabicyclo[5.4.0]undec-7-ene (DBU, 0.180 g, 0.177 mL, 1.20 mmol) was added to the above solution, and the solution was stirred at rt for 10 h. The crude product was concentrated under reduced pressure and purified by column chromatography (SiO_2) using toluene/CH_3OH (97:3, v/v) to afford **14** as a brown solid in 23% yield (0.065 g). ^{1}H NMR ($CDCl_3$), δ, ppm: 8.45 (br, J = 8.8 Hz, 4H, $\underline{H}_o$); 8.22 (br, J = 8.5 Hz, 2H, $\underline{H}_4$ and $\underline{H}_7$); 8.05 (br, J = 8.5 Hz, 2H, $\underline{H}_3$ and $\underline{H}_8$); 7.70 (s, 2H, $\underline{H}_5$ and $\underline{H}_6$); 7.10 (br, J = 8.8 Hz, 4H, $\underline{H}_m$); 4.7−4.0 (br, 8H, O−C$\underline{H}_2$−C$\underline{H}_2$−O); 3.80 (br, 4H, O−C$\underline{H}_2$−CH_3); 1.30 (br, 6H, O−CH_2−C$\underline{H}_3$). MALDI-TOF: found 1485.9 $[M + H]^+$, calculated 1484.2 for $C_{102}H_{40}N_2O_{12}$.

Rotaxane 1. Fulleromacrocycle **11** (0.013 g, 0.01 mmol) and $[Cu(CH_3CN)_4][PF_6]$ (0.0038 g, 0.01 mmol) were placed in a round bottomed flask under N_2 atmosphere. A mixture composed of CH_2Cl_2 and CH_3CN (3 mL, 3:1) was added by syringe. The solution was stirred at room temperature under N_2 atmosphere for 30 min. Ferrocene thread **10** (0.0113 g, 0.01 mmol) in dry CH_2Cl_2 (1 mL) was added dropwise by syringe. The mixture was then stirred for another 2 h at room temperature. The solvent was removed under reduced pressure, followed by column chromatography (SiO_2) using CH_2Cl_2/CH_3OH (97:3, v/v) as eluent to yield the desired rotaxane **1** as a brown solid in 53% yield (0.014 g). ^{1}H NMR ($CDCl_3$), δ, ppm: 8.56 (d, J = 8.6 Hz, 2H, H_4' and H_7'); 8.40 (d, J = 8.6 Hz, 2H, H_4 and H_7); 8.21 (s, 2H, H_5' and H_6'); 7.99 (d, J = 8.3 Hz, 4H, ferrocene ortho Ar-$\underline{H}$); 7.90 (s, 2H, H_5 and H_6); 7.89 (d, J = 8.6 Hz, 2H, H_3' and H_8'); 7.75 (d, J = 8.6 Hz, 2H, H_3 and H_8); 7.46 (d, J = 8.3 Hz, 4H, ferrocene meta Ar-$\underline{H}$); 7.60 (d, J = 8.8 Hz, 4H, H_o'); 7.37 (d, J = 8.8 Hz, 4H, H_o); 6.03 (d, J = 8.8 Hz, 4H, H_m'); 5.90 (d, J = 8.8 Hz, 4H, H_m); 4.94 (br, 2H, Cp-$\underline{H}$); 4.40 (br, 2H, Cp-$\underline{H}$); 4.25 (br, 5H, Cp-$\underline{H}$); 4.00−3.50 (m, 32H, O−C$\underline{H}_2$−C$\underline{H}_2$−O). MALDI-TOF: *m*/*z* found 2505.29 $[M - PF_6]^+$, calculated, 2650.23 for $C_{161}H_{86}N_4O_{16}Fe_2CuPF_6$.

Rotaxane 2. This rotaxane was prepared from thread **10** and macrocycle **14** following the same procedure described for rotaxane **1**. Brown solid, 23% yield (0.007 g). ^{1}H NMR ($CDCl_3$), δ, ppm: 8.59 (br, J = 8.6 Hz, 2H, H_4' and H_7'); 8.43 (br, J = 8.6 Hz, 2H, H_4 and H_7); 8.24 (br, 2H, H_5' and H_6'); 7.96 (br, J = 8.3 Hz, 4H, ferrocene ortho Ar-$\underline{H}$); 7.91 (br, 2H, H_5 and H_6); 7.88 (br, J = 8.6 Hz, 2H, H_3' and H_8'); 7.75 (br, J = 8.6 Hz, 2H, H_3 and H_8); 7.46 (br, J = 8.3 Hz, 4H, ferrocene meta Ar-$\underline{H}$); 7.60 (br, J = 8.8 Hz, 4H, H_o'); 7.37 (br, J = 8.8 Hz, 4H, H_o); 6.03 (br, J = 8.8 Hz, 4H, H_m'); 5.90 (br, J = 8.8 Hz, 4H, H_m); 4.94 (br, 2H, Cp-$\underline{H}$); 4.40 (br, 2H, Cp-$\underline{H}$); 4.25 (br, 5H, Cp-$\underline{H}$); 4.00−3.50 (br, 32H, O−C$\underline{H}_2$−C$\underline{H}_2$−O) 3.30 (br, 4H, O−C$\underline{H}_2$−CH_3); 1.30 (br, 6H, O−CH_2−C$\underline{H}_3$). MALDI-TOF: *m*/*z* found 2880 $[M - PF_6]^+$, calculated, 3025.14 for $C_{168}H_{96}N_4O_{20}Fe_2CuPF_6$.

Rotaxane 3.[14c] In the reaction flask, macrocycle **17** (0.060 g, 0.0425 mmol) was dissolved in 5 mL of degassed CH_2Cl_2/CH_3CN (7:3, v/v) to which $[Cu(CH_3CN)_4][PF_6]$ (0.016 g, 0.0425 mmol) was added under N_2 atmosphere. The dark orange solution was stirred for 30 min at rt. The diazidophenanthroline ligand **16** (0.029 g, 0.0425 mmol) was then added as a solid to the flask and the deep red solution was stirred under N_2 at rt for 3 h to afford precursor **18**. Meanwhile, CuI (0.017 g, 0.089 mmol), sodium ascorbate (0.07 g, 0.353 mmol), and sulfonated bathophenanthroline (0.100 g, 0.17 mmol) were added to 5 mL of a degassed solvent mixture composed of H_2O/EtOH (1:1, v/v) under N_2 atmosphere. The suspension was heated to reflux for 2 min, cooled to rt and added by syringe to the flask containing **18**. Finally, ethynyl ferrocene (0.026 g, 0.127 mmol, added as a solid) and DBU (0.019 g, 19 μL, 0.127 mmol) were added and the red mixture was stirred under N_2 for 12 h at rt. The crude mixture was neutralized by adding 2 mL of 10%

HCl aqueous solution and extracted with CH_2Cl_2 (3 × 50 mL). The organic phase was washed with water (3 × 50 mL), concentrated to a volume of 10 mL and then stirred for 2 h with saturated MeOH solution of KPF_6 to effect the anion exchange. The solvents were evaporated under reduced pressure, and the remaining insoluble light brown solid was extracted with CH_2Cl_2 (3 × 100 mL) and then filtered through paper. The solvent was evaporated under reduced pressure, and the crude product was purified by flash chromatography (SiO_2) first using CH_2Cl_2 to elute unreacted ethynyl ferrocene and then CH_2Cl_2/CH_3OH (97:3, v/v) to afford rotaxane **3** as a brown solid in 92% yield (0.025 g).^{1}H NMR ($CDCl_3$), δ, ppm: 8.56 (d, J = 8.6 Hz, 2H, H_4' and H_7'); 8.40 (d, J = 8.6 Hz, 2H, H_4 and H_7); 8.21 (s, 2H, H_5' and H_6'); 7.93 (s, 2H, H_5 and H_6); 7.89 (d, J = 8.6 Hz, 2H, H_3' and H_8'); 7.75 (d, J = 8.6 Hz, 2H, H_3 and H_8); 7.75 (s, 2H, H-triazole ring); 7.60 (d, J = 8.8 Hz, 4H, H_o'); 7.37 (d, J = 8.8 Hz, 4H, H_o); 6.03 (d, J = 8.8 Hz, 4H, H_m'); 5.90 (d, J = 8.8 Hz, 4H, H_m); 4.94 (br, 2H, Cp-H); 4.82 (br, 4H, O−CH_2−CH_2−OOC); 4.52 (m, 4H, CH_2-triazole ring); 4.40 (br, 2H, Cp-H); 4.25 (br, 5H, Cp-H); 4.00−3.50 (m, 36H, O−CH_2−CH_2−O). MALDI-TOF: m/z found 2577.36 [M − PF_6]$^+$, calculated, 2722 for $C_{159}H_{98}N_{10}O_{16}Fe_2CuPF_6$.

Rotaxane Model 4. This rotaxane was prepared from thread **10** and a phen-based methyl benzoate ester macrocycle, which was prepared in accordance to our previous works,[14b,c] following the same procedure described for rotaxane **1**. Red solid, 66% yield (0.013 g). ^{1}H NMR ($CDCl_3$), δ, ppm: 8.53 (d, J = 8.6 Hz, 2H, H_4' and H_7'); 8.46 (d, J = 8.6 Hz, 2H, H_4 and H_7); 8.20 (s, 2H, H_5' and H_6'); 7.96 (d, J = 8.3 Hz, 4H, ferrocene ortho Ar-H); 7.93 (s, 2H, H_5 and H_6); 7.89 (d, J = 8.6 Hz, 2H, H_3' and H_8'); 7.77 (d, J = 8.6 Hz, 2H, H_3 and H_8); 7.41 (d, J = 8.3 Hz, 4H, ferrocene meta Ar-H); 7.60 (d, J = 8.8 Hz, 4H, H_o'); 7.37 (d, J = 8.8 Hz, 4H, H_o); 6.96 (d, 2H, ester-containing ortho Ar-H); 6.66 (d, 1H, ester-containing para Ar-H); 6.03 (d, J = 8.8 Hz, 4H, H_m'); 5.90 (d, J = 8.8 Hz, 4H, H_m); 4.94 (br, 2H, Cp-H); 4.40 (br, 2H, Cp-H); 4.25 (br, 5H, Cp-H); 4.00−3.50 (m, 35H, O−CH_2−CH_2−O and COOCH_3). MALDI-TOF: m/z found 1851.18 [M − PF_6]$^+$, calculated 1996.45 for $C_{106}H_{92}N_4O_{16}CuFe_2PF_6$.

Rotaxane Model 5. This rotaxane was prepared from thread **16** and a phen-based methyl benzoate ester macrocycle, which was prepared in accordance to our previous works,[14b,c] following the same procedure described for rotaxane **3**. Red solid, 94% yield (0.019 g). ^{1}H NMR ($CDCl_3$), δ ppm: 8.63 (d, J = 8.6 Hz, 2H, H_4' and H_7'); 8.48 (d, J = 8.6 Hz, 2H, H_4 and H_7); 8.26 (s, 2H, H_5' and H_6'); 7.85 (s, 2H, H_5 and H_6); 7.81 (d, J = 8.6 Hz, 2H, H_3' and H_8'); 7.78 (s, 2H, H-triazole ring); 7.75 (d, J = 8.6 Hz, 2H, H_3 and H_8); 7.60 (d, J = 8.8 Hz, 4H, H_o'); 7.37 (d, J = 8.8 Hz, 4H, H_o); 6.90 (d, 2H, ester-containing ortho Ar-H); 6.62 (d, 1H, ester-containing meta Ar-H); 6.09 (d, J = 8.8 Hz, 4H, H_m'); 5.90 (d, J = 8.8 Hz, 4H, H_m); 4.94 (br, 2H, Cp-H); 4.52 (m, 4H, CH_2-triazole); 4.40 (br, 2H, Cp-H); 4.25 (br, 5H, Cp-H); 4.00−3.50 (m, 47H, O−CH_2−CH_2−O and COOCH_3). MALDI-TOF: m/z found 1937.18 [M − PF_6]$^+$, calculated 2082.45 for $C_{105}H_{106}N_{10}O_{16}CuFe_2PF_6$.

Acknowledgment. Support of the work at NYU by grants from the National Science Foundation and by a research fund established by former members of the Schuster group is gratefully appreciated. This investigation was conducted in part using an instrumental facility at NYU constructed with support from Research Facilities Improvement Grant Number C06 RR-16572-01 from the National Center for Research Resources, National Institutes of Health. We also thank the Deutsche Forschungsgemeinschaft (SFB 583), FCI and Office of Basic Energy Sciences of the U.S. Department of Energy for financial support. G.M. thanks the von Humboldt Foundation for financial support.

Supporting Information Available: Synthesis and structural data of rotaxanes **1**−**6** and **14**. ^{1}H NMR spectra of **1**, **3**, **4**, **6**, **13**, **14**, **16**, and **17**. MALDI-TOF spectra of **5** and **14**. This material is available free of charge via the Internet at http://pubs.acs.org.

References and Notes

(1) Portions of this work were published in preliminary form without experimental details in: Schuster, D. I.; Li, K.; Guldi, D. *C. R. Chim.* **2006**, *9*, 892–908. Some of the data reported here, obtained subsequently using improved instrumentation, differ to some extent from data reported in the 2006 publication.

(2) *Supramolecular Chemistry - Concepts and Perspectives*; Lehn, J.-M., Ed.; Wiley-VCH: Weinheim, Germany, 1995.

(3) (a) Cram, D. J. *Science* **1983**, *219*, 1177–1181. (b) Lehn, J.-M. *Science* **1985**, *227*, 849–856. (c) Philp, D.; Stoddart, J. F. *Angew. Chem., Int. Ed. Engl.* **1996**, *35*, 1155–1196. (d) Gates, B. D.; Xu, Q.; Stweart, M.; Ryan, D.; Willson, C. G.; Whitesides, G. M. *Chem. Rev.* **2005**, *105*, 1171–1196.

(4) (a) *The Photosynthetic Bacterial Reaction Center. Structure and Dynamics*; Breton, J., Vermeglio, H., Eds.; Plenum: New York, 1988. (b) *Supramolecular Photochemistry*; Balzani, V., Scandola, F., Eds.; Horwood: Chichester, U.K., 1991. (c) Sauvage, J.-P.; Collin, J.-P.; Chambron, J.-C.; Guillerez, S.; Coudret, C.; Baltani, V.; Barigelletti, F.; De Cola, L.; Flamigni, L. *Chem. Rev.* **1994**, *94*, 993–1019. (d) Gust, D.; Moore, T. A.; Moore, A. L. *Acc. Chem. Res.* **1993**, *26*, 198–205.

(5) For few representative examples, see: (a) Collin, J.-P.; Harriman, A.; Heitz, V.; Odobel, F.; Sauvage, J.-P. *J. Am. Chem. Soc.* **1994**, *116*, 5679–5690. (b) Sandanayaka, A. S. D.; Watanabe, N.; Ikeshita, K.; Araki, Y.; Kihara, N.; Furusho, Y.; Ito, O.; Takata, T. *J. Phys. Chem. B* **2005**, *109*, 2516–2525. (c) Hagemann, O.; Jørgensen, M.; Krebs, F. C. *J. Org. Chem.* **2006**, *71*, 5546–5559. (d) Sgobba, V.; Giancane, G.; Conoci, S.; Casilli, S.; Ricciardi, G.; Guldi, D. M.; Prato, M.; Valli, L. *J. Am. Chem. Soc.* **2007**, *129*, 3148–3156. (e) Figueira-Duarte, T.; Lloveras, V.; Vidal-Gancedo, J.; Gegout, A.; Delavaux, N. B.; Welter, R.; Veciana, J.; Rovira, C.; Nierengarten, J. F. *Chem Commum.* **2007**, *42*, 4345–4347. (f) Regehly, M.; Ermilov, E. A.; Helmreich, M.; Hirsch, A.; Jux, N.; Roeder, B. *J. Phys. Chem. B* **2007**, *111*, 998–1006. (g) Santos, J.; Grim, B.; Islescas, B. M.; Martin, N. *Chem. Commun.* **2008**, *45*, 5993. (h) Santos, J.; Grimm, B.; Illescas, B. M.; Guldi, D. M.; Martin, N. *Chem. Commum.* **2008**, *45*, 5993–5995. (i) Sarova, G. H.; Hartnagel, U.; Balbinot, D.; Sali, S.; Jux, N.; Hirsch, A.; Guldi, D. M. *Chem.*−*Eur. J.* **2008**, *14*, 3137–3145. (j) Gayathri, S. S.; Wielopolski, M.; Perez, E. M.; Fernandez, G.; Sanchez, L.; Viruela, R.; Orti, E.; Guldi, D. M.; Martin, N. *Angew. Chem., Int. Ed.* **2009**, *48*, 815–819. (k) Stoddart., J. F. *Chem. Soc. Rev.* **2009**, *38*, 1802–1820. (l) Kira, A.; Umeyama, T.; Matano, Y.; Yoshida, K.; Isoda, S.; Park, J.; Kang, K.; Imahori, H. *J. Am. Chem. Soc.* **2009**, *131*, 3198–3200.

(6) (a) Balzani, V.; Juris, A.; Venturi, M.; Campagna, S.; Serroni, S. *Chem. Rev.* **1996**, *96*, 759–833. (b) Indelli, M. T.; Scandola, F.; Flamigni, L.; Collin, J.-P.; Sauvage, J.-P.; Sour, A. *Inorg. Chem.* **1997**, *36*, 4247–4250. (c) Serroni, S.; Campagna, S.; Puntoriero, F.; Di Pietro, C.; McClenaghan, N. D.; Loiseau, F. *Chem. Soc. Rev.* **2001**, *30*, 367–375. (d) Armaroli, N. *Photochem. Photobiol. Sci.* **2003**, *2*, 73–87.

(7) For some examples, see: (a) Armaroli, N.; Diederich, F.; Echegoyen, L.; Habicher, T.; Flamigni, L.; Marconi, G.; Nierengarten, J. F. *New J. Chem.* **1999**, *23*, 77–83. (b) Dixon, I. M.; Collin, J.-P.; Sauvage, J.-P.; Barigelletti, F.; Flamigni, L. *Angew. Chem., Int. Ed.* **2000**, *39*, 1292–1296. (c) Daros, T.; Prato, M.; Guldi, D. M.; Ruzzi, M.; Pasimeni, L. *Chem.*−*Eur. J.* **2001**, *7*, 816–820. (d) D'Souza, F.; Deviprasad, G. R.; El-Khouly, M. E.; Fujitsuka, M.; Ito, O. *J. Am. Chem. Soc.* **2001**, *123*, 5277–5284. (e) Wilson, S. R.; MacMahon, S.; Tat, F. T.; Jarowski, P. D.; Schuster, D. I. *Chem. Commun.* **2003**, 226–229. (f) Rio, Y.; Enderlin, G.; Bourgogne, C.; Nierengarten, J. F.; Gisselbrecht, J. P.; Gross, M.; Accorsi, G.; Armaroli, N. *Inorg. Chem.* **2003**, *42*, 8783–8793. (g) Imahori, H.; Fukuzumi, S. *Adv. Func. Mater.* **2004**, *14*, 525–536.

(8) For some examples see: (a) Livoreil, A.; Sauvage, J.-P.; Armaroli, N.; Balzani, V.; Flamigni, L.; Ventura, B. *J. Am. Chem. Soc.* **1997**, *119*, 12114–12124. (b) Sauvage, J.-P.; Dietrich-Buchecker, C. O. *Molecular Catenanes, Rotaxanes and Knots*; Wiley-VCH: Weinheim, Germany, 1999. (c) Balzani, V.; Credi, A.; Venturi, M. *Molecular Devices and Machines-A Journey into the Nano World*; Wiley-VCH: Weinheim, Germany, 2003. (d) Thordarson, P.; Bijsterveld, J. A.; Rowan, A. E.; Nolte, R. J. M. *Nature* **2003**, *424*, 915–918. (e) Badijic, J. D.; Credi, V.; Silvi, S.; Stoddart, J. F. *Science* **2004**, *303*, 1845–1849. (f) Serrel, V.; Lee, C.-F.; Kay, E. R.; Leigh, D. A. *Nature* **2005**, *445*, 523–527. (g) Green, J. E.; Choi, J. W.; Boukai, A.; Bunimovich, Y.; Johnston-Halperin, E.; Delonno, E.; Luo, Y.; Scheriff,

B. A.; Xu, K.; Shin, Y. S.; Tseng, H.-R.; Stoddart, J. F.; Heath, J. R. *Nature* **2007**, *445*, 414–417. (h) Lee, C. F.; Leigh, D. A.; Pritchard, R. G.; Schultz, D.; Teat, S. J.; Timco, G. A.; Winpenny, R. E. P. *Nature* **2009**, *458*, 314–318.

(9) (a) Li, K.; Schuster, D. I.; Guldi, D. M.; Herranz, M. A.; Echegoyen, L. *J. Am. Chem. Soc.* **2004**, *126*, 3388–3389. (b) Li, K.; Bracher, P. J.; Guldi, D. M.; Herranz, M. A.; Echegoyen, L.; Schuster, D. I. *J. Am. Chem. Soc.* **2004**, *126*, 9156–9157. (c) Schuster, D. I.; Li, K.; Guldi, D. M.; Ramey, J. *Org. Lett.* **2004**, *6*, 1919–1922.

(10) (a) Dietrich-Buchecker, C. O.; Sauvage, J.-P. *Tetrahedron Lett.* **1983**, *24*, 5095–5098. (b) Dietrich-Buchecker, C. O.; Sauvage, J.-P. *J. Am. Chem. Soc.* **1984**, *106*, 3043–3044. (c) Dietrich-Buchecker, C. O.; Sauvage, J.-P. *Chem. Rev.* **1987**, *87*, 795–810. (d) Dietrich-Buchecker, C. O.; Sauvage, J.-P. *Tetrahedron* **1990**, *46*, 503–512.

(11) Bao, D.; Millare, B.; Xia, W.; Steyer, B. G.; Gerasimenko, A. A.; Ferreira, A.; Contreras, A.; Vulley, V. I. *J. Phys. Chem. A* **2009**, *113*, 1259–1267.

(12) For some representative examples, see: (a) Guldi, D. M.; Maggini, M.; Scorrano, G.; Prato, M. *J. Am. Chem. Soc.* **1997**, *119*, 974–980. (b) Imahori, H.; Yamada, H.; Nishimura, Y.; Yamazaki, I.; Sakata, Y. *J. Phys. Chem. B* **2000**, *104*, 2099–2108. (c) Imahori, H.; Norieda, H.; Yamada, H.; Nishimura, Y.; Yamazaki, I.; Sakata, Y.; Fukuzumi, S. *J. Am. Chem. Soc.* **2001**, *123*, 100–110. (d) Imahori, H.; Tamaki, K.; Guldi, D. M.; Luo, C.; Fujitsuka, M.; Ito, O.; Sakata, Y.; Fukuzumi, S. *J. Am. Chem. Soc.* **2001**, *123*, 2607–2617. (e) Fujitsuka, M.; Tsuboya, N.; Hamasaki, R.; Ito, M.; Onodera, S.; Ito, O.; Yamamoto, Y. *J. Phys. Chem. A* **2003**, *107*, 1452–1458. (f) Gonzalez-Rodriguez, D.; Torres, T.; Olmstead, M. M.; Rivera, J.; Angeles-Herranz, M.; Echegoyen, L.; Atienza, C. C.; Guldi, D. M. *J. Am. Chem. Soc.* **2006**, *128*, 10680–10681. (g) Mateo-Alonso, A.; Ehli, C.; Rahman, G. M. A.; Guldi, D. M.; Fioravanti, G.; Marcaccio, M.; Paolucci, F.; Prato, M. *Angew. Chem., Int. Ed. Engl.* **2007**, *46*, 3521–3525. (h) Marois, J.-S.; Cantin, K.; Desmarais, A.; Morin, J.-F. *Org. Lett.* **2008**, *10*, 33–36. (i) Marczak, R.; Wielopolski, M.; Gayathri, S. S.; Guldi, D. M.; Matsuo, Y.; Matsuo, K.; Tahara, K.; Nakamura, E. *J. Am. Chem. Soc.* **2008**, *130*, 16207–16215. (j) Spaenig, F.; Kovacs, C.; Hauke, F.; Ohkubo, K.; Fukuzumi, S.; Guldi, D. M.; Hirsch, A. *J. Am. Chem. Soc.* **2009**, *131*, 8180–8195.

(13) (a) Huisgen, R. *Angew. Chem., Int. Ed. Engl.* **1968**, *80*, 321–328. (b) Kolb, H. C.; Finn, M. G.; Sharpless, K. B. *Angew. Chem., Int. Ed. Engl.* **2001**, *40*, 2004–2021. (c) Tornøe, C. W.; Christensen, C.; Meldal, M. *J. Org. Chem.* **2002**, *67*, 3057–3064.

(14) (a) Megiatto, J. D., Jr.; Schuster, D. I. *J. Am. Chem. Soc.* **2008**, *130*, 12872–12873. (b) Megiatto, J. D., Jr.; Schuster, D. I. *Chem.—Eur. J.* **2009**, *15*, 5444–5448. (c) Megiatto, J. D., Jr.; Spencer, R.; Schuster, D. I. *Org. Lett.* **2009**, *11*, 4152–4155. (d) Megiatto, J. D., Jr.; Schuster, D. I. *New J. Chem.* **2010**, *34*, 276–286.

(15) DIC = *N*,*N*′-diisopropylcarbodiimide, DMAP = 4-(dimethylamino)pyridine and EDC = 1-ethyl-3-(3-(dimethylamino)propyl)carbodiimide.

(16) (a) Nierengarten, J.-F.; Habicher, T.; Kessinger, R.; Cardullo, F.; Diederich, F.; Gramlih, V.; Gisselbrecht, J.-P.; Boudon, C.; Gross, M. *Helv. Chim. Acta* **1997**, *80*, 2238–2276. (b) *Fullerenes*; Hirsch, A., Brettreich, M., Eds.; Wiley-VCH: Weinheim, Germany, 2005.

(17) All pseudorotaxane (or "nonstoppered" rotaxane) model compounds used in this work were freshly prepared because they are not stable species and may undergo unthreading on standing. For details, see ref 9.

(18) (a) Flamigni, L.; Talarico, A. M.; Chambron, J.-C.; Heitz, V.; Linke, M.; Fujita, N.; Sauvage, J.-P. *Chem.—Eur. J.* **2004**, *10*, 2689–2699. (b) Periyasamy, G.; Sour, A.; Collin, J.-P.; Sauvage, J.-P.; Remacle, F. *J. Phys. Chem. B* **2009**, *113*, 6219–6229.

(19) (a) Prato, M.; Guldi, D. M. *Acc. Chem. Res.* **2000**, *33*, 695–703. (b) Guldi, D. M. *Chem. Soc. Rev.* **2002**, *31*, 22–36.

(20) In benzonitrile, two processes were detected. We are not sure about the nature of the second process. However, the most probable explanation to us seems to be a conformational rearrangement of the phenanthroline ligand, due to the oxidation of Cu(I) to Cu(II).

(21) A longer lived minor component with a lifetime of 7.9 μs is also detected.

(22) Implementation of the solvent correction term to adjust for the energy of solvation by benzonitrile is expected to minimally affect these energy values.

(23) In a recent study of an $Al^{III}P-C_{60}-Fc$ triad, electron transfer from Fc to the oxidized porphyrin was invoked, even though the lifetime of the charge-separated state of the triad was lower, not higher, than that of the corresponding dyad. See: Poddutoori, P. K.; Sandanayaka, A. S. D.; Hasobe, T.; Ito, O.; van der Est, V. *J. Phys. Chem. B*, doi: 10.1021/jp911937d.

(24) Schuster, D. I.; Megiatto, J. D., Jr.; Guldi, D. M.; Rojas, G.; Abwandner, S. Unpublished results, manuscript in preparation.

JP101154K